Fusion energy production from a deuterium-tritium plasma in the JET tokamak

1992 Nucl. Fusion 32 187

(http://iopscience.iop.org/0029-5515/32/2/I01)

FUSION ENERGY PRODUCTION FROM A DEUTERIUM-TRITIUM PLASMA IN THE JET TOKAMAK

JET Team*
JET Joint Undertaking,
Abingdon, Oxfordshire,
United Kingdom

ABSTRACT. The paper describes a series of experiments in the Joint European Torus (JET), culminating in the first tokamak discharges in deuterium-tritium fuelled mixtures. The experiments were undertaken within limits imposed by restrictions on vessel activation and tritium usage. The objectives were: (i) to produce more than one megawatt of fusion power in a controlled way; (ii) to validate transport codes and provide a basis for accurately predicting the performance of deuterium-tritium plasmas from measurements made in deuterium plasmas; (iii) to determine tritium retention in the torus systems and to establish the effectiveness of discharge cleaning techniques for tritium removal; (iv) to demonstrate the technology related to tritium usage; and (v) to establish safe procedures for handling tritium in compliance with the regulatory requirements. A single-null X-point magnetic configuration, diverted onto the upper carbon target, with reversed toroidal magnetic field was chosen. Deuterium plasmas were heated by high power, long duration deuterium neutral beams from fourteen sources and fuelled also by up to two neutral beam sources injecting tritium. The results from three of these high performance hot ion H-mode discharges are described: a high performance pure deuterium discharge; a deuterium-tritium discharge with a 1% mixture of tritium fed to one neutral beam source; and a deuterium-tritium discharge with 100% tritium fed to two neutral beam sources. The TRANSP code was used to check the internal consistency of the measured data and to determine the origin of the measured neutron fluxes. In the best deuterium-tritium discharge, the tritium concentration was about 11% at the time of peak performance, when the total neutron emission rate was 6.0×10^{17} neutrons/s. The integrated total neutron yield over the high power phase, which lasted about 2 s, was 7.2×10^{17} neutrons, with an accuracy of $\pm 7\%$. The actual fusion amplification factor, Q_{DT}, was about 0.15. With an optimum tritium concentration, this pulse would have produced a fusion power of ≈ 5 MW and a nominal $Q_{DT} \approx 0.46$. The same extrapolation for the pure deuterium discharge would have given ≈ 11 MW and a nominal $Q_{DT} = 1.14$, so that the total fusion power (neutrons and α-particles) would have exceeded the total losses in the equivalent deuterium-tritium discharge in these transient conditions. Techniques for introducing, tracking, monitoring and recovering tritium were demonstrated to be highly effective: essentially all of the tritium introduced into the neutral beam system and, so far, about two thirds of that introduced into the torus have been recovered.

1. INTRODUCTION

The essential objective of JET, as defined in 1975 [1], is to obtain and study a plasma in conditions and dimensions approaching those needed in a thermonuclear reactor. These studies are aimed at defining the parameters, the size and the working conditions of a tokamak reactor. The realization of this objective involves four main areas of work:

(1) the scaling of plasma behaviour as parameters approach the reactor range;
(2) the plasma-wall interaction in these conditions;
(3) the study of plasma heating; and
(4) the study of α-particle production, confinement and consequent plasma heating.

Extensive studies have been made in the first and third areas of work: reactor relevant temperatures (up to 30 keV), densities (up to 4×10^{20} m^{-3}) and energy confinement times (up to 1.7 s) have been achieved in separate discharges [2–4].

The second area of work has been well covered in the limiter configuration for which JET was originally designed. However, the highest performance JET discharges have been obtained with a 'magnetic limiter', that is in the so-called X-point configuration with a magnetic separatrix inside the vacuum vessel, with plasma contacting localized areas of the wall (the X-point targets) and detached from the limiters except during the formation of the discharge. The duration of the high performance phase of these discharges can exceed 1.5 s; this is achieved by careful design of the targets and specific operational techniques, but is limited, ultimately, by an unacceptably high influx

* See Annex.

of impurities, characterized by a rapid increase in electron density, effective ionic charge and radiated power which is referred to in this paper as the 'carbon bloom'. This has been demonstrated in other discharges to be associated with overheating of the target surfaces [5]. For a reactor, new solutions to this problem are required. This is the motivation for the planned reconstruction of the interior of the JET vacuum vessel to provide a pumped divertor duct (or channel) which will allow controlled dissipation of the escaping power flux and better screening of the plasma from wall produced impurities [6].

The fourth area of work has been started by earlier studies of energetic particles produced as fusion products or by ion cyclotron resonance heating (ICRH). It is now addressed further by the first tokamak plasma experiments in deuterium-tritium mixtures. The fusion reactions studied are listed in the Appendix. The high performance achieved in deuterium discharges, together with the experience gained in making substantial modifications to JET in a beryllium environment and with significant vessel activation[1], gave confidence that an experiment with about 10% of tritium in the plasma could be performed and would provide data that can be used to plan an effective campaign of deuterium-tritium experiments in 1996.

This paper describes a series of experiments, culminating in the deuterium-tritium experiment, with the following objectives:

- To produce in excess of one megawatt of fusion power in a controlled way;
- To validate transport codes and provide a basis for accurately predicting the performance of deuterium-tritium plasmas from measurements made in deuterium plasmas [7]; to establish for these plasmas the consistency of different experimental measurements; and to calibrate diagnostics;
- To determine tritium retention in the torus walls and the neutral beam injection (NBI) system; and to establish the effectiveness of various discharge cleaning techniques for tritium removal;
- To demonstrate the technology related to tritium usage (tritium NBI, cryopumping and tritium handling);
- To establish safe procedures for handling tritium in compliance with the regulatory requirements.

[1] The precautions required for working in this environment (for example ventilated suits) are similar to those required in a tritium environment.

2. EXPERIMENTAL ARRANGEMENT

2.1. Overall limitations to operation

To perform a deuterium-tritium experiment at this stage in the JET programme, it was necessary to limit the total neutron production to less than about 1.5×10^{18} neutrons so that the resulting vessel activation would be compatible with the modification work on the pumped divertor scheduled for 1992/1993. In addition, the total amount of tritium available was restricted to $\simeq 0.2$ g ($\simeq 2000$ Ci)[2] since the JET tritium processing plant is not scheduled to come into operation until 1993. Taken together, these limitations restricted, to a few, the total number of high performance discharges in this series of experiments.

2.2. First wall materials and discharge preparation

The interior of the JET vacuum vessel, shown in Fig. 1, consists of: a continuous top X-point target, comprising plates clad with carbon fibre composite (CFC) tiles; a continuous bottom X-point target clad with beryllium tiles; and a pair of outer wall toroidal belt limiters above and below the midplane, the upper one of beryllium and the lower one of carbon. All other plasma contacting surfaces, such as the inner wall, are of CFC, graphite or beryllium. The two target plates were carefully aligned to avoid discontinuities and, in addition, the individual tiles were carefully shaped to minimize the effect of residual protrusions and steps, which were about one millimetre.

The plasma contacting surfaces were extensively conditioned by a combination of glow discharge cleaning and tokamak discharge operation. Before the introduction of tritium, all the plasma contacting components were coated with beryllium by periodically evaporating beryllium inside the vacuum vessel. A fresh layer was deposited about twelve hours before the deuterium-tritium experiment.

2.3. Choice of discharge type and magnetic configuration

A range of possible JET discharge types was, in principle, suitable for the deuterium-tritium experiment. However, pellet fuelling was excluded, since the present pellet injector was not designed to operate with deuterium-tritium plasmas. Furthermore, ICRH,

[2] 1 Ci = 3.7×10^{10} Bq or 37 GBq.

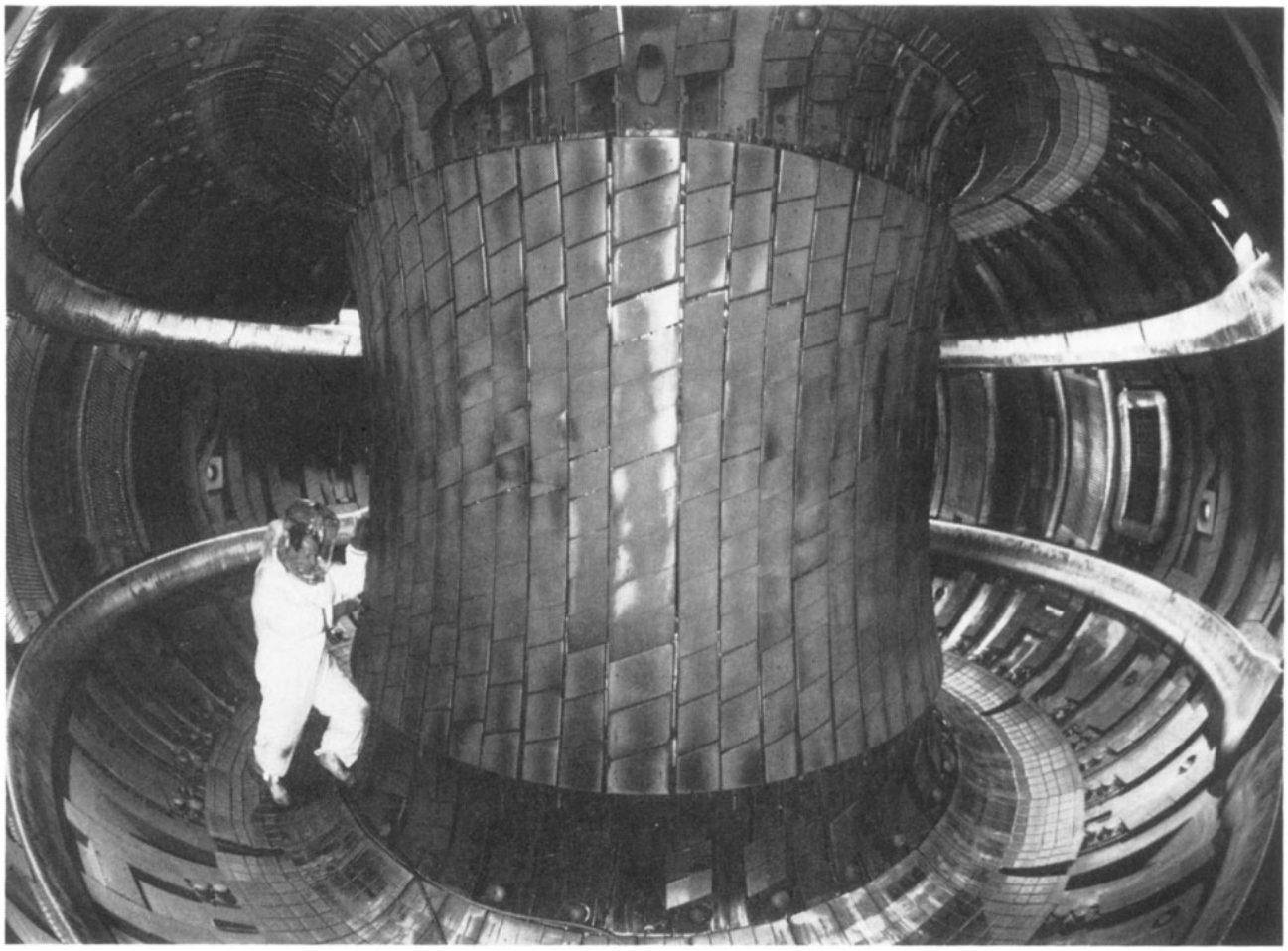

FIG. 1. Interior of the JET vacuum vessel.

although available, was not used in order to avoid introducing tritium into the absorption pumps on the power feed lines. Consequently, attention concentrated on discharges heated by NBI. The highest neutron emission rates were obtained in hot ion discharges (at low density, with the ion temperature significantly higher than the electron temperature) in the H-mode regime (X-point discharges with improved confinement above an input power threshold) [8]. An attempt was made to identify such a discharge with good performance and reproducibility, and with relative insensitivity to small changes, for instance in the level of injected power.

During the series of experiments leading to the deuterium–tritium experiment, plasmas with similar performance were achieved in both double-null X-point configurations (which took advantage of both the top and the bottom X-point targets) and single-null X-point configurations (which use only the top X-point target). Ultimately, a single-null X-point discharge, diverted onto the upper carbon target, with reversed toroidal magnetic field, was chosen. In this configuration (shown in Fig. 2), ions drift away from the target towards the plasma. This has been found to lead to a more equal power loading between the inner and outer branches of the X-point [5]. Overall, this configuration allows consistently higher energy input and longer duration of the high performance phase of the discharge before the 'carbon bloom' (see Section 4).

2.4. Tritium introduction by neutral beam injection

Neutral beam injection is an effective way of introducing tritium into the type of discharge selected for the deuterium–tritium experiment. It ensures that tritium reaches the hot, dense centre of the discharge

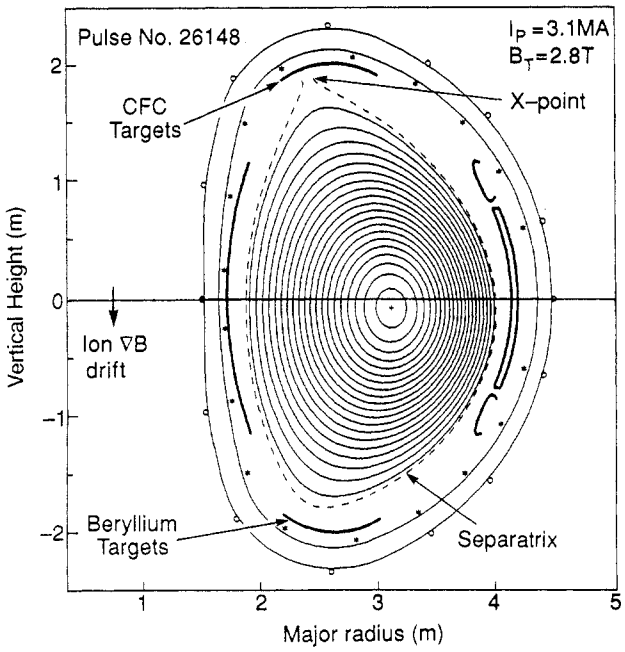

FIG. 2. Magnetic configuration for pulse No. 26148 in which the magnetic axis is at R_{mag} = 3.15 m, the horizontal minor radius a = 1.05 m and the safety factor q_{cyl} = 2.8. At the 95% flux surface, the elongation κ = 1.6 and the surface q_ψ = 3.8. Shown are the separatrix, the X-point, the ion ∇B drift direction and the carbon fibre composite (CFC) and beryllium targets.

TABLE I. TRITIUM NBI CHARACTERISTICS FOR ONE PINI

Acceleration voltage	78 kV
Injected neutral species mix	Power fraction
78 kV	79%
39 kV	12%
26 kV	9%
Equivalent atomic current	12 A
Power injected	0.75 MW
Tritium gas requirement for 2 s injected pulse	45 mb·L (i.e. 120 Ci or 0.012 g)

where the reactivity is highest and so minimizes the amount of tritium which needs to be injected into the torus. For the deuterium-tritium experiment, tritium gas was supplied from a uranium storage bed and a buffer reservoir through a pressure regulator and needle valve and introduced into the neutralizers of two of the sixteen JET positive ion neutral injection sources (PINIs) (Fig. 3(a) and (b)). The tritium gas introduction system was enclosed in a secondary containment system. Approximately 6% of the tritium taken from the uranium storage bed was injected into the plasma as energetic neutrals; most of the tritium was collected on the cryopanels and ion beam dumps in the NB vacuum system and was subsequently recovered (see Section 6). This is the first time that an NB system was used to inject energetic tritium neutrals at high power and long pulse duration into a fusion plasma and represents an important advance in this technology.

The characteristics of each tritium PINI, given in Table I, are those used in the deuterium-tritium experiment. The PINIs were deliberately operated below maximum performance to ensure high reliability. To conserve the limited amount of tritium available, the change from deuterium to tritium in these PINIs was simulated in the NB test bed using hydrogen and deuterium gas. Consequently, before the deuterium-tritium pulses, only two 1.5 s tritium conditioning pulses were needed to change the beams from deuterium to tritium.

For the deuterium-tritium experiment, the remaining fourteen PINIs were operated in deuterium: twelve at 135 kV, delivering ≈10.5 A each (total power ≈10.7 MW, with power fractions of 59%, 21% and 20%), and two at 75 kV, delivering ≈19 A each (total power ≈2.1 MW, with power fractions of 73%, 17% and 10%); the total deuterium fuelling rate was 164 A. The tritium fuelling rate relative to the total was ≈13% with two tritium PINIs.

2.5. Tritium gas introduction and recovery systems

In this programme of deuterium-tritium experiments, it was important to demonstrate the reliable and efficient operation of tritium NBI and to gain experience both in handling, injecting and monitoring the usage of tritium and in recovering tritium from the torus and the NB systems.

To collect and measure the injected tritium, the normal torus backing pump system was replaced by a cryogenic gas collection system, enclosed within a secondary containment system. This is shown schematically in Fig. 3(c). During operation, the gas flow

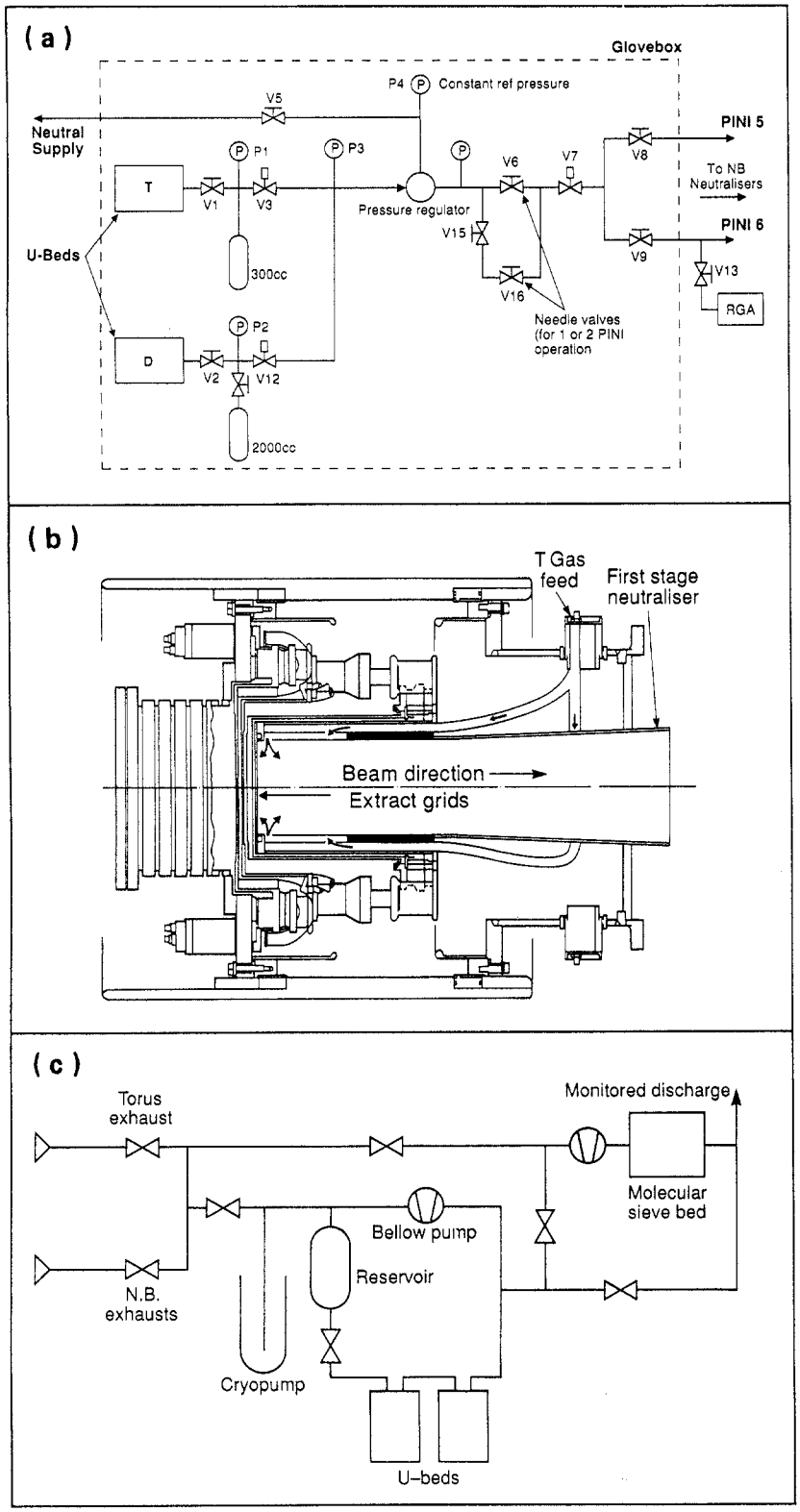

FIG. 3. (a) Tritium gas introduction system, (b) tritium feed to the NB neutralizer and (c) tritium gas collection system.

from the torus condensed on a tubular cryopump containing activated charcoal at liquid helium temperature. Subsequently, the condensed tritium, together with larger amounts of deuterium, was transferred to uranium storage beds for retrieval and separation at a future date. After the experiment, the NB cryopanels were warmed to release cryocondensed gas, which was then collected in the cryogenic system in a similar way. The system was equipped with ion current collectors which could be operated either as absolutely calibrated gauges for tritium [9] or as ionization chambers. The exhaust gases from both the torus and the NB systems were sampled for analysis and tritium assay, and monitored before discharge to ensure compliance with statutory requirements. Using these techniques, the time dependent recovery of tritium from the torus and NB systems was assessed (see Section 6).

2.6. Diagnostic capability

More than thirty diagnostics were in operation for the deuterium-tritium experiment.

The time dependent neutron emission rates were measured with silicon surface barrier diodes (which exploited the high threshold energy of (n, p) and (n, α) nuclear reactions in silicon and recorded 14 MeV neutrons) and using ^{235}U and ^{238}U fission chambers (which were not capable of discriminating between 2.5 MeV and 14 MeV neutrons). These detectors were calibrated by comparison with the total time integrated neutron yield derived from the activation of two small samples of silicon positioned in a vacuum vessel port with an unobstructed view of the plasma. Just before a discharge, the samples were put in place by a pneumatic system. Silicon was selected for its short decay half-life (which allows the samples to be recycled between discharges), but, since the $^{28}Si(n,p)$ reaction cross-sections are not well known, it was necessary to cross-calibrate against the standard dosimetry reactions $^{63}Cu(n, 2n)^{62}Cu$ and $^{56}Fe(n, p)^{56}Mn$ using samples at other positions. The neutron fluence at each measurement position was related to the total neutron yield from the plasma through extensive and detailed neutron transport calculations. The accuracy of the total neutron yield is estimated to be $\pm 7\%$.

The neutron spectrum was measured with a liquid scintillator spectrometer. A flat pulse height distribution is obtained up to the maximum energy corresponding to the complete transfer of neutron energy to the recoiling proton. Neutron emission profile data can be obtained from 19 similar spectrometers arranged in two cameras with orthogonal views of a vertical section of plasma. 2.5 MeV and 14 MeV neutrons are distinguished, except when high fluxes of 14 MeV neutrons inhibit the measurement of low fluxes of 2.5 MeV neutrons.

Other essential diagnostics [10] included magnetic measurements (used to determine the equilibrium configuration and the plasma energy referred to here as diamagnetic energy), electron cyclotron emission (for the electron temperature T_e), an infrared interferometer (for the electron density n_e), LIDAR Thomson scattering (for T_e and n_e), active charge exchange recombination spectroscopy (for the ion temperature T_i and impurity concentrations) and visible bremsstrahlung (for the line of sight averaged effective ionic charge $\bar{Z}_{eff}$).

2.7. Data consistency

In planning and executing the deuterium-tritium experiment, the TRANSP code [11] was used to check the internal consistency of the measured data and to estimate the fraction of neutrons which were produced by thermal-thermal, beam-thermal and beam-beam reactions on the basis of the measured profiles of n_e, T_e and T_i and the measured Z_{eff} with an assumed flat profile. In particular, measurement and simulation were compared for the diamagnetic energies, the loop voltage and, most importantly, the neutron emission rates. An important advantage of the TRANSP code is its treatment of neutral injection physics using Monte Carlo techniques to determine, for example, the ion and electron heating and the neutron emission rates due to NBI.

3. EXPERIMENTAL RESULTS

The results from three discharges in the series of experiments, culminating in the deuterium-tritium experiment, will be described. The first is the best of several similar high performance pure deuterium discharges (pulse No. 26087), the second is a deuterium-tritium discharge with a 1% mixture of tritium in deuterium introduced into one PINI (pulse No. 26095 is one of three similar discharges) and the third is a deuterium-tritium discharge with a 100% tritium gas feed into two PINIs (pulse No. 26148 is one of two similar discharges). In all cases, the plasma current, which started to increase at a time t = 0, is maintained at a 'flat-top' in excess of 3 MA from 5 s to 15 s and then decreased towards zero, which is reached near 25 s.

TABLE II. MAIN PLASMA PARAMETERS FOR DEUTERIUM PULSE No. 26087 AND DEUTERIUM-TRITIUM PULSE Nos 26095 AND 26148

Parameter	Units	Pulse No. 26087	Pulse No. 26095	Pulse No. 26148
Time (t)	s	13.35	13.7	13.25
Plasma current (I_p)	MA	3.1	3.1	3.1
Toroidal field (B_T)	T	2.8	2.8	2.8
NB power (P_{NB})	MW	14.9	14.2	14.3
Volume averaged electron density ($\langle n_e \rangle$)	10^{19} m^{-3}	3.5	3.3	2.5
Central electron density ($\hat{n}_e$)	10^{19} m^{-3}	5.1	4.5	3.6
Volume averaged (D + T) density ($\langle n_D \rangle + \langle n_T \rangle$)	10^{19} m^{-3}	2.9	2.5	1.6
Central (D + T) density ($\hat{n}_D + \hat{n}_T$)	10^{19} m^{-3}	4.1	3.4	2.4
Line averaged effective charge ($\bar{Z}_{eff}$)		1.8	2.2	2.4
Average electron temperature $\langle T_e \rangle$	keV	5.6	6.1	6.0
Central electron temperature ($\hat{T}_e$)	keV	10.5	11.9	9.9
Average ion temperature ($\langle T_i \rangle$)	keV	6.7	7.4	8.0
Central ion temperature ($\hat{T}_i$)	keV	18.6	22.0	18.8
Plasma diamagnetic energy (W_{dia})	MJ	11.6	11.2	9.1
(dW_{dia}/dt)[a]	MW	6.0	3.9	4.7
Ratio of plasma pressure to toroidal field pressure (β_T)	%	2.2	2.2	1.7
Ratio of plasma pressure to poloidal field pressure (β_p)		0.83	0.80	0.64
Ratio to Troyon limit (β_T/β_{Troy})[b]		0.8	0.8	0.6
Energy replacement time (τ_E)[a,c]	s	1.2	1.0	0.9
Fusion triple product ($(\hat{n}_D + \hat{n}_T)\hat{T}_i\tau_E$)[a]	10^{20} m^{-3}·keV·s	9.0	7.5	3.8
Ratio of average T to (D + T) density[d] $(\langle n_T \rangle/(\langle n_D \rangle + \langle n_T \rangle))$	%	0	0.08	11
Ratio of central T to (D + T) density[d] $(\hat{n}_T/(\hat{n}_D + \hat{n}_T))$	%	0	0.08	10
Maximum total neutron emission rate	10^{17} s^{-1}	0.43	0.49	6.0
Total neutron yield	10^{17}	0.55	0.70	7.2
Q[e]		5.1×10^{-3}	6.5×10^{-3}	0.15

[a] Calculated from averages over the previous 0.2 s.
[b] β_{Troy} (%) = $g_N \mu_0 I_p$[MA]/B_T[T]a[m], where a is the horizontal minor radius, g_N = 2.2, and μ_0 = 0.4 π in these units.
[c] $\tau_E = W_{dia}/(P_{tot} - dW_{dia}/dt)$.
[d] From TRANSP simulation.
[e] Definition of Q similar to that of Q_{DT}.

3.1. Pure deuterium discharge

Figure 4 shows the time development of a number of characteristic parameters during the current 'flat-top' of pulse No. 26087, including the central temperatures, average density, $\bar{Z}_{eff}$, plasma diamagnetic energy and total neutron emission rates. The plasma target for NBI is formed by allowing the density to fall during the transition from a limiter configuration to an X-point configuration. The result is a moderately peaked density profile. At 12 s, the NB power increases to $\approx$15 MW, which leads, after 0.3 s, to the transition to the H-mode phase of the discharge. During the subsequent 1 s, sawteeth are stabilized and the centrally peaked NB heating produces peaked temperature profiles. The ion and electron temperatures rise continuously throughout this phase, reaching 18.6 keV and 10.5 keV, respectively. The plasma diamagnetic energy

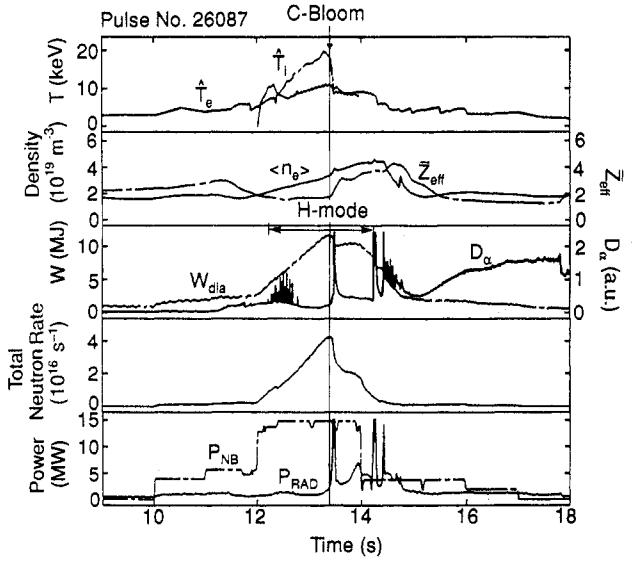

FIG. 4. Time development of the central electron and ion temperatures, the volume averaged electron density, the line averaged $\bar{Z}_{eff}$, the plasma diamagnetic energy, the D_α emission, the total neutron emission rate, and the NB power and radiated power for pulse No. 26087.

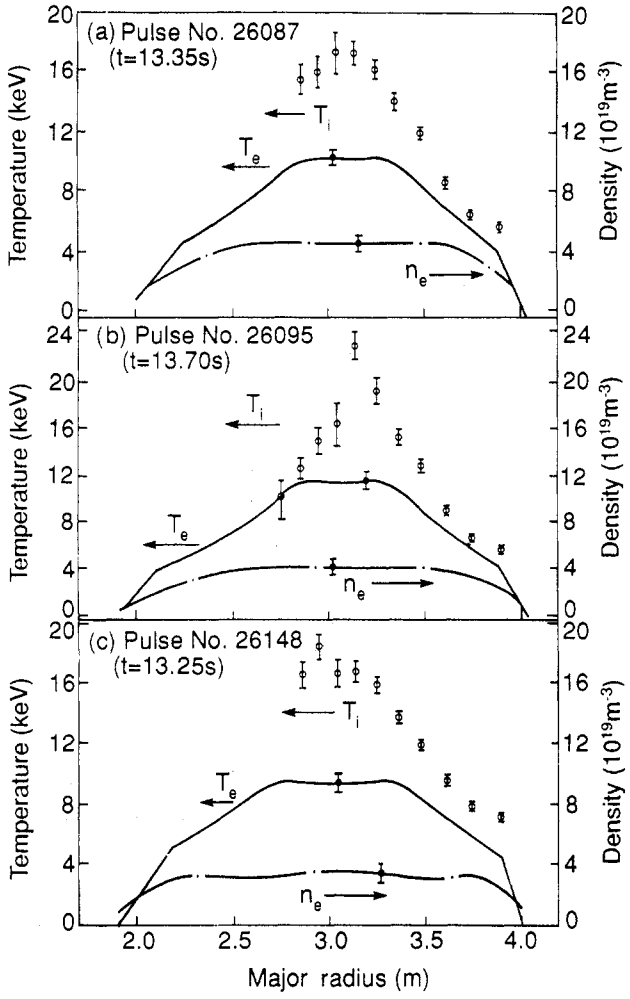

FIG. 5. Radial profiles of the ion and electron temperatures and the electron density for (a) pulse No. 26087, (b) pulse No. 26095 and (c) pulse No. 26148.

reaches 11.6 MJ, corresponding to a ratio of plasma pressure to magnetic pressure of 2.2%. The main plasma parameters at this time are listed in Table II and the plasma profiles are shown in Fig. 5(a). As the central plasma pressure rises and energetic NB ions accumulate in the plasma centre, 'fishbone'-like oscillations grow. However, these have no obvious effect on the energetic ions and neutrons or the discharge performance. The high performance phase is terminated at a time (13.4 s) characterized by a rise in edge emission from D_α and C III (the 'carbon bloom'), followed by a sawtooth collapse of the central plasma temperatures. Nevertheless, the H-mode persists until the high power NBI is switched off at 14 s. The time development of these discharges is typical of hot ion H-modes with their characteristically long sawtooth free periods of up to 1.5 s.

The consistency of the data is demonstrated by the good agreement obtained between the measured and simulated emission rates for 2.5 MeV neutrons (see Fig. 6). The simulation also showed that $\approx 60\%$ of the neutrons were produced by thermal–thermal reactions, while the remainder were mostly produced by beam–thermal reactions, with only a small fraction produced by beam–beam reactions.

3.2. Discharge with 1% tritium in one PINI

Figure 7 shows the time development of the characteristic parameters for pulse No. 26095. All of these increase throughout the phase of the discharge which starts at 12.3 s and ends with a 'carbon bloom' at 13.7 s. The main plasma parameters at this time are listed in Table II and the plasma profiles are shown in Fig. 5(b).

Again, the consistency of the data is demonstrated by the good agreement obtained between the measured and the simulated neutron emission rates. In this case, the comparison is made for both 2.5 MeV and 14 MeV neutrons (see Fig. 8) and indicates that the diagnostics

and the TRANSP code are well calibrated by these measurements. The simulations showed that ≈50% of the neutrons were produced by thermal–thermal reactions, while the remainder were mostly produced by beam–thermal reactions, with only a small fraction produced by beam–beam reactions.

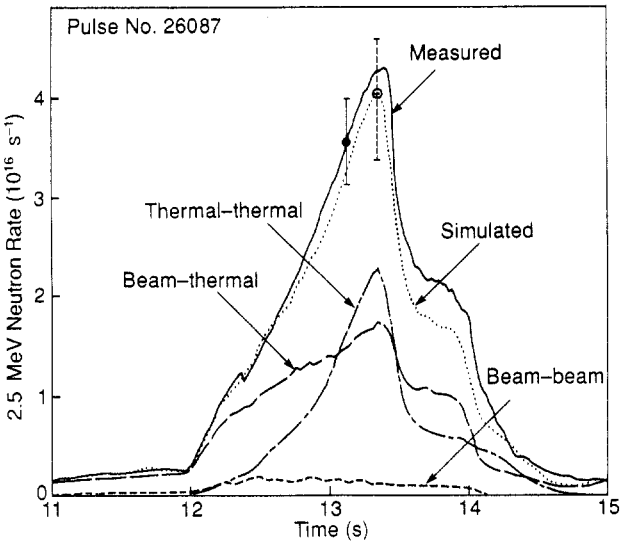

FIG. 6. Fission chamber measurements and TRANSP simulations of 2.5 MeV neutron rates for pulse No. 26087.

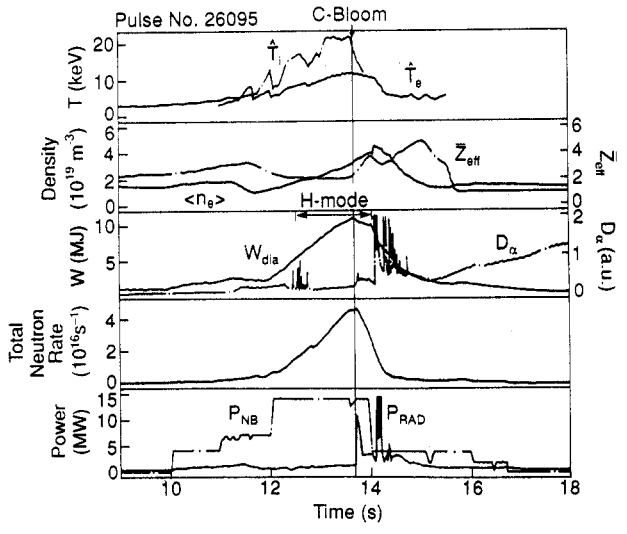

FIG. 7. Time development of the central electron and ion temperatures, the volume averaged electron density, the line averaged $\bar{Z}_{eff}$, the plasma diamagnetic energy, the D_α emission, the total neutron emission rate, and the NB power and radiated power for pulse No. 26095.

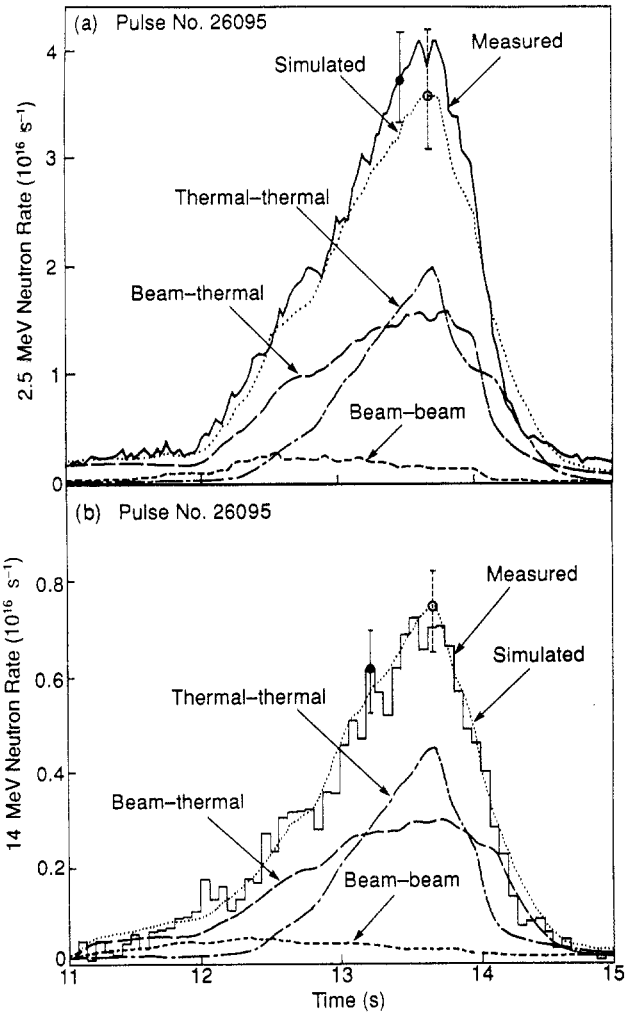

FIG. 8. For pulse No. 26095, (a) fission chamber measurements and TRANSP simulations of 2.5 MeV neutron rates, and (b) silicon diode measurements and TRANSP simulations of 14 MeV neutron rates.

Specific experiments aimed at measuring the transport of thermalized tritium and deuterium were performed in discharges similar to pulse No. 26095, but these experiments still require detailed analysis and will be reported in a subsequent publication.

3.3. Discharge with 100% tritium gas feed to two PINIs

To minimize activation levels and tritium usage, only two pulses of this type were attempted. The two were similar and each produced fusion power in excess of 1.5 MW. The neutral beam power versus time

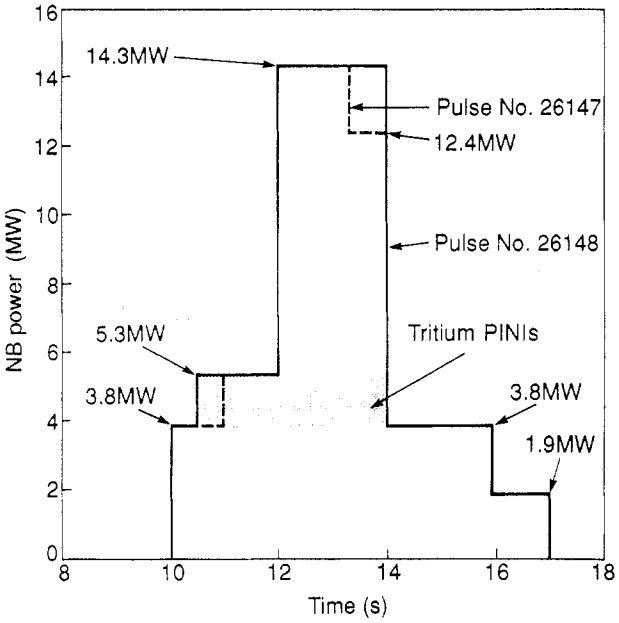

FIG. 9. Neutral beam power versus time for pulse No. 26147 and pulse No. 26148.

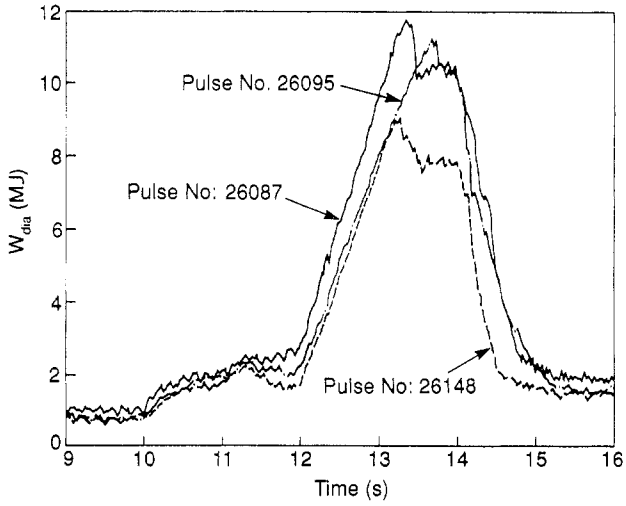

FIG. 11. Time development of the diamagnetic energy W_{dia} for pulses Nos 26087, 26095 and 26148.

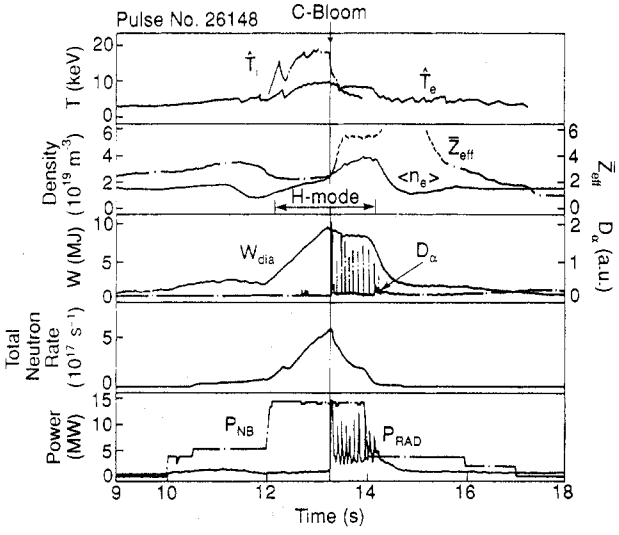

FIG. 10. Time development of the central electron and ion temperatures, the volume averaged electron density, the line averaged $\bar{Z}_{eff}$, the plasma diamagnetic energy, the D_α emission, the total neutron rate, and the NB and radiated power for pulse No. 26148. After the 'carbon bloom', the Z_{eff} measurement (....) is affected by black body radiation emanating from the targets.

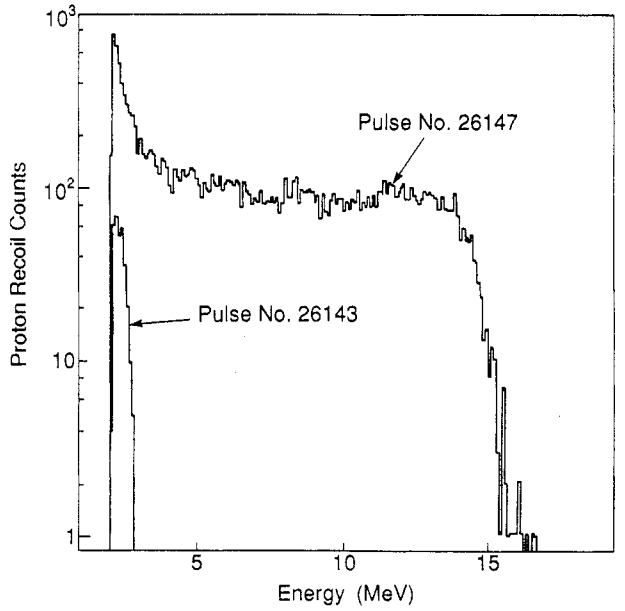

FIG. 12. Proton recoil pulse height spectrum for the deuterium–tritium pulse No. 26147 (predominantly 14 MeV neutrons) and the deuterium pulse No. 26143 (2.5 MeV neutrons only).

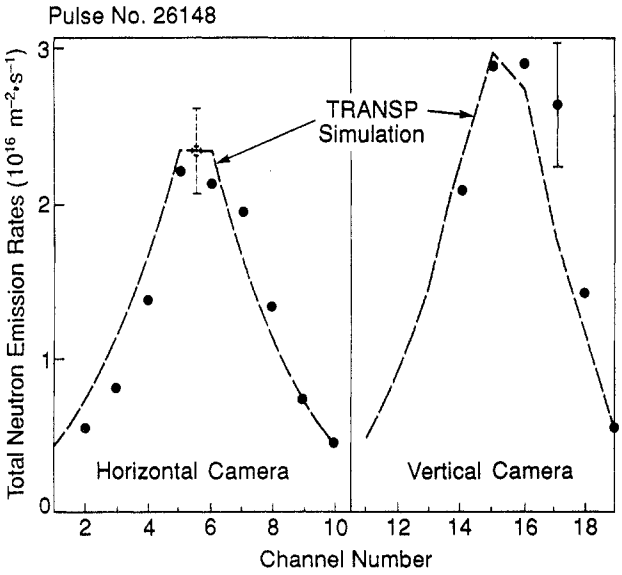

FIG. 13. Measured and simulated neutron emission (14 MeV neutrons) integrated along particular lines of sight as measured by the horizontal (channels 2–10) and vertical (channels 14–19) cameras for pulse No. 26148.

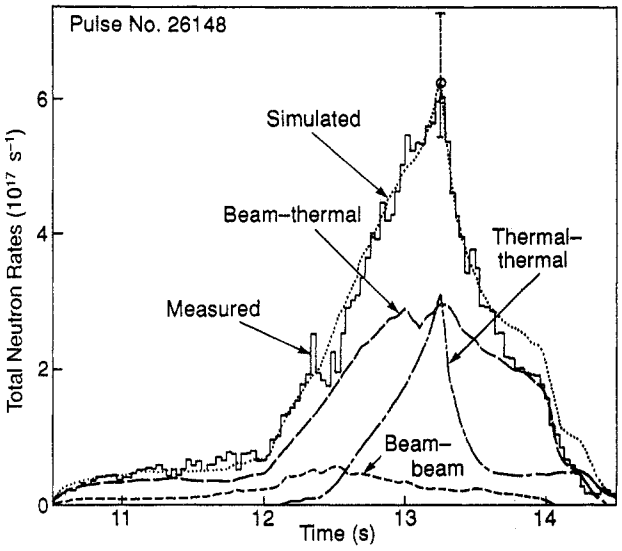

FIG. 14. Silicon diode measurements and TRANSP simulations of the total neutron rates (predominantly 14 MeV neutrons) for pulse No. 26148.

(shown schematically in Fig. 9) was chosen by selecting the switch-on time of pairs of PINIs. The full curve corresponds to pulse No. 26148 (which had 1.5 s tritium pre-fuelling) and the dashed curve corresponds to pulse No. 26147 (which had 1 s tritium pre-fuelling). These times were chosen to give effective fuelling, as predicted by the TRANSP code and confirmed by the results of discharges with 1% tritium in one PINI. These discharges were also heated by up to four deuterium PINIs, before and after high power heating. This suppressed MHD instabilities at early times and secured a disruption free decay of the plasma current at late times. In pulse No. 26147, two deuterium PINIs were switched off at 13.2 s.

Figure 10 shows the time development of the characteristic parameters for pulse No. 26148. All of these increase throughout the phase of the discharge which starts at 12.4 s and ends with a 'carbon bloom' at 13.3 s. The main plasma parameters are listed in Table II and the plasma profiles are shown in Fig. 5(c).

Figure 11 compares the time development of the plasma diamagnetic energy in pulses Nos 26087, 26095 and 26148. For the two discharges with the same total input power (pulses Nos 26095 and 26148) the time development is very similar until the earlier onset of the 'carbon bloom' at 13.3 s in pulse No. 26148 (see Section 4), when the plasma energy was 9.1 MJ. In pulse No. 26095, the plasma energy increased to 11.2 MJ at the time of the 'carbon bloom' at 13.7 s. The plasma diamagnetic energy was even higher in pulse No. 26087, both at the start and the termination of the H-mode. Furthermore, the fusion triple product for this pulse is about twice that for pulse No. 26148 in which the hydrogen isotope density is lower because of the lower electron density and the higher Z_{eff} (see Table II).

The proton recoil pulse height spectrum for pulse No. 26147 (Fig. 12) shows clearly the presence of 14 MeV neutrons. The total emission is about forty times that obtained for 2.5 MeV neutrons in a similar deuterium discharge (pulse No. 26143). The 14 MeV neutrons, which interact with carbon nuclei in the scintillator, also give rise to the high emission observed at a few MeV.

The line integrated neutron emission rates, as measured by the horizontal and vertical cameras of the neutron profile monitor and normalized to the 14 MeV neutron emission rates obtained from the fission chambers, show good agreement with the results of TRANSP simulations (Fig. 13). The peaks are displaced by ≈ 0.1 m, but this is well within the uncertainties of the simulation. More detailed studies, including improvements to the somewhat idealized geometries used, are in progress.

The consistency of the data is again demonstrated by the good agreement obtained between the measured and simulated emission of 14 MeV neutrons (see Fig. 14). Again, the simulations showed that $\approx 50\%$ of

the neutrons were produced by thermal–thermal reactions, while the remainder were mostly produced by beam–thermal reactions, with only a small fraction produced by beam–beam reactions. The peak total neutron emission rate was 6.0×10^{17} neutrons/s in a high power phase lasting about 2 s. The integrated total neutron yield was 7.2×10^{17} neutrons, with an accuracy of $\pm 7\%$. The total fusion releases (α-particles and neutrons) were 1.7 MW of peak power and 2 MJ of energy.

The simulation also gave the α-particle characteristics listed in Table III. Clearly, the level of α-particle heating was too low, in comparison with the NB power, to have a discernible effect on the electron temperature. Furthermore, the α-particle pressure and concentration were probably too low for the stimulation of collective effects, although, as no detailed studies have been made, these effects cannot be excluded entirely.

TABLE III. ALPHA PARTICLE CHARACTERISTICS FROM THE TRANSP SIMULATION OF PULSE No. 26148 AT 13.2 s (instantaneous equilibration model for α-particles)

Overall power transfers	
From α-particles to electrons	260 kW
From α-particles to ions	60 kW
From NB to electrons	1.8 MW
From NB to ions	9.4 MW
NB loss by shinethrough	0.4 MW
NB loss by charge exchange	1.5 MW
Equipartition of ions to electrons	2 MW
Central power transfers	
From α-particles to electrons	13 kW/m^3
From α-particles to ions	3.6 kW/m^3
From NB to electrons	75 kW/m^3
From NB to ions	610 kW/m^3
Central α-particle concentrations	
Ratio of α-particle pressure to thermal plasma pressure	$\approx 4\%$
Ratio of α-particle pressure to total plasma pressure	$\approx 2.5\%$
Ratio of α-particle density to electron density	$\approx 0.08\%$

However, the characteristics of the MHD activity observed in the two tritium discharges were very similar to those of pure deuterium discharges such as pulse No. 26087.

Since the deuterium and tritium source rates were similarly peaked on axis, the two mixing models described in Ref. [7] for deuterium and tritium (i.e. identical radial profiles or equal velocities) resulted in similar deuterium and tritium profiles and gave an equally good fit to the neutron data.

4. DISCHARGE TERMINATION AND VARIABILITY

The high performance discharges, typical of the experiments reported in Section 3, were limited by the 'carbon bloom'. The time at which this occurred affected the maximum neutron emission rates as shown in Fig. 15 and, for a given magnetic configuration, was principally dependent on the level and duration of heating, characterized in Ref. [12] by the total energy, E_C, conducted to the X-point targets:

$$E_C = \int_{t_{X\text{-point}}}^{t_{bloom}} \left(P_{tot} - P_{rad} - \frac{dW}{dt} \right) dt$$

where P_{tot} is the total input power, P_{rad} is the radiated power and dW/dt is the rate of change of plasma energy.

For the particular configuration, power and pulse duration in these experiments, the 'carbon bloom' occurred when E_C was typically 11 ± 3 MJ. In some cases, this occurred 'naturally', presumably due to the progressive rise of the target temperature. In other cases, when the conducted energy was in this range, the 'carbon bloom' could be triggered by an MHD event, such as a giant edge localized mode (ELM) or a sawtooth collapse which coupled to an ELM. The occurrence of these events appears to depend upon the precise time evolution of the plasma density and the additional heating and showed some variability in these experiments.

In comparison with other similar discharges in deuterium, the high performance phase of the deuterium–tritium pulses Nos 26147 and 26148 terminated as a result of a somewhat earlier sawtooth collapse, coupled to an ELM, leading to the 'carbon bloom' (1.3 s after the start of full NB power, see Fig. 10 for pulse No. 26148). Detailed analysis of the collapse showed that the inversion radius of such sawteeth was no larger than that of normal sawteeth. However, strong

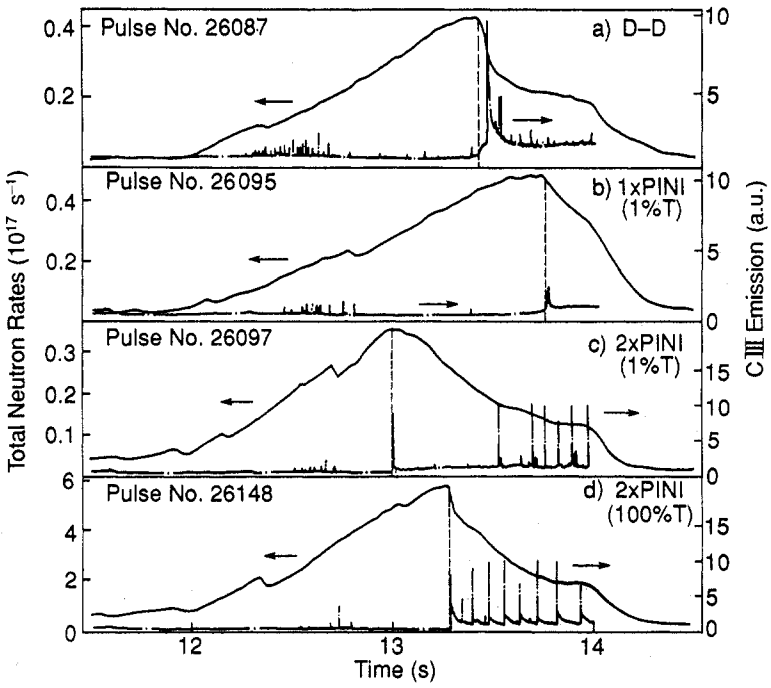

FIG. 15. Variation in the time of termination of the high performance phase of a number of similar discharges as shown by the fall in the neutron emission rate. The dashed vertical lines show the time of the 'carbon bloom' as characterized by increased emission of C III light from the plasma edge. In (a) and (b) the bloom occurs 'naturally', in (c) it is triggered by an ELM, and in (d) it is triggered by a sawtooth collapse coupled to an ELM.

coupling between central and edge modes was observed and might have played a role in triggering the ELM, which occurred within 100 μs of the sawtooth collapse.

5. EXTRAPOLATION TO FULL PERFORMANCE DEUTERIUM-TRITIUM DISCHARGES

A global measure of performance is given by a fusion amplification factor, Q_{DT}, defined as the sum of separate terms arising from thermal-thermal, Q_{tt}, beam-thermal, Q_{bt}, and beam-beam, Q_{bb}, reactions:

$$Q_{DT} = Q_{tt} + Q_{bt} + Q_{bb}$$

where $Q_{tt} = P_{tt}/(P_{loss} - 0.2\,P_{tt})$

$Q_{bt} = P_{bt}/(P_b - P_{st})$

$Q_{bb} = P_{bb}/(P_b - P_{st})$

P_{tt}, P_{bt} and P_{bb} are the total fusion powers, respectively, from thermal-thermal, beam-thermal and beam-beam reactions, $P_{loss} = P_b + P_\Omega - P_{st} - dW/dt + P_{\alpha x}$ is the total power lost from the plasma (including radiation and charge exchange), and P_b, P_Ω, P_{st}, dW/dt and $P_{\alpha x}$ are, respectively, the NB input power, the Ohmic input power, the power lost by NB 'shinethrough', the rate of change of plasma diamagnetic energy, and the actual experimentally achieved α-power.

With this definition it is easy to evaluate Q_{DT} for an actual plasma using the separation into thermal-thermal, beam-thermal and beam-beam powers given by the TRANSP code. At the time of peak neutron emission in pulse No. 26148, Q_{DT} determined in this way is 0.15.

To estimate the value of Q_{DT} which would be obtained for a similar discharge but with a more optimal deuterium-tritium mixture, a nominal Q_{DT} is defined as the value that would be obtained if the hydrogen isotope content of the actual plasma were replaced instantaneously by the more optimal mixture with a tritium concentration, $c = \langle n_T \rangle / (\langle n_D \rangle + \langle n_T \rangle)$. At the times of peak neutron emission, and with $c = 0.6$ (chosen for maximum fusion power, including the beam thermal part), the nominal Q_{DT} value is 0.46

in the deuterium–tritium pulse No. 26148 and 1.14 in the deuterium pulse No. 26087.

This nominal Q_{DT} value is very similar to that which would have been obtained experimentally if eight of the sixteen PINIs (instead of two in pulse No. 26148 and none in pulse No. 26087) had been used to inject tritium into a 50:50 deuterium–tritium target plasma. In this case, TRANSP simulations of these two pulses, with the actual plasma conditions and NB power, and with acceleration voltages used in the experiment, give $Q_{DT} = 0.44$ for pulse No. 26148 and $Q_{DT} = 1.07$ for pulse No. 26087 (in each case the value of c is determined by NBI and is about 0.5). The total fusion power (neutrons and α-particles) and the fraction coming from thermal–thermal reactions for the two pulses would be 4.6 MW (43%) and 9.6 MW (57%), respectively.

In relating these extrapolations to what should be possible in JET in the future, it should be remembered that, for the main deuterium–tritium experiments foreseen for 1996, there will be 12.5 MW of tritium NBI at a principal energy of 160 kV, and 8 MW of deuterium NBI at a principal energy of 140 kV. The higher power and the better beam penetration should give higher values of Q_{DT}. It should also be possible to use up to 20 MW of ICRH, either alone or in combination with NB heating, in which case the total fusion power should also increase, but with little increase in Q_{DT}. Experiments with the pumped divertor are expected to control impurities, avoiding or, at least, delaying the 'bloom' and giving a cleaner plasma, which should lead to a further increase in Q_{DT}.

6. TRITIUM CLEAN-UP EXPERIMENTS

6.1. Recovery of tritium from the torus

It was anticipated that full recovery of tritium from the large surface area of the torus would be relatively difficult, and controlled clean-up experiments were performed to assess the effectiveness of various discharge techniques in removing tritium.

The total amount of tritium injected into the torus was 53 ($\pm$4) Ci. In the 36 hours between the last tritium pulse No. 26148 and the start of the cleanup experiments, about 15 Ci were recovered onto the tubular cryopump by pumping alone. The detailed results of these experiments will be reported elsewhere. Provisionally, measurements showed that the tritium concentration in successive clean-up discharges fell in accordance with a multi-reservoir development of the two-reservoir model [13] established on the basis of data from hydrogen and deuterium discharges. In the course of 25 pulses, the amount of tritium released within 40 min of a pulse fell from 1 Ci per pulse to 0.1 Ci per pulse. Pulses which contacted different parts of the torus wall were used to remove tritium which, at least after the first few clean-up pulses, was distributed over the walls. A soak with D_2 gas after a series of pulses typically removed $\approx$0.1 Ci. Nine days after the deuterium–tritium experiment, and after $\approx$100 pulses of various types, the tritium removal rate was $\approx$0.02 Ci per pulse. Three weeks after the experiment, the removal rate was 3 mCi per pulse, and the total amount of tritium remaining in the torus walls was $\approx$15 ($\pm$10) Ci, about one third of that injected. These results will be confirmed when the vacuum vessel is entered and the tritium content of the wall tiles is analysed.

6.2. Recovery of tritium from the NB system

Measurements on the tritium gas introduction system showed that 1000 ($\pm$100) Ci were extracted from the uranium storage bed and introduced into the NB system for pulses Nos 26147 and 26148, of which 53 ($\pm$4) Ci were estimated to have been injected into the torus. Following the deuterium–tritium experiment, the neutral beams were injected into the beam calorimeters with the NB system valved off from the torus. Neutron counter measurements showed that essentially all the tritium on the beam dumps was desorbed in a small number of pulses, corresponding to the fluence of each PINI for about 100 s. Monitoring the regeneration of the NB cryopumps through the gas collection system then showed that, within the accuracy of the measurements ($\sim$10%), essentially all the tritium in the NB system was recovered. After a further regeneration and warming to room temperature, subsequent regenerations released only a few curies from the NB system.

7. SUMMARY AND CONCLUSIONS

In JET, high performance deuterium discharges with $Q_{DD} > 2 \times 10^{-3}$ and nominal $Q_{DT} > 0.5$ are obtained routinely and reliably. The best JET deuterium pulse gave $Q_{DD} = 5 \times 10^{-3}$ and a nominal $Q_{DT} = 1.14$, so that the total fusion power (neutrons and α-particles) would exceed the total losses in the equivalent deuterium–tritium discharge in these transient conditions.

For the first time, experiments on a high fusion performance tokamak plasma have been made using a deuterium–tritium fuel mixture. An equivalent tritium neutral current of 24 A was injected into a deuterium plasma, heated by deuterium neutral beams. The tritium concentration was about 11% at the time of peak performance when the total neutron emission rate was 6.0×10^{17} neutrons/s. The integrated total neutron yield over the high power phase, which lasted about 2 s, was 7.2×10^{17} neutrons, with an accuracy of ±7%. The total fusion releases were 1.7 MW at peak power and 2 MJ of energy. The amount of tritium injected and the number of discharges with tritium were deliberately restricted for operational convenience.

The consistency of the experimental data was established with simulations using the TRANSP code, which showed, in particular, that thermal–thermal and beam–thermal reactions contributed about equally to the total neutron emission.

The good agreement obtained between measurement and simulation gave confidence in the accuracy of extrapolations from existing discharges. Assuming a tritium concentration $c = \langle n_T \rangle / (\langle n_D \rangle + \langle n_T \rangle) = 0.6$ (the optimum for fusion power output), the deuterium–tritium pulse No. 26148 would have produced a fusion power of ≈5 MW and a nominal $Q_{DT} \approx 0.46$. The same extrapolation for the pure deuterium pulse No. 26087 would have given ≈11 MW and a nominal $Q_{DT} = 1.14$. Use of the more optimum NB system intended for JET in 1996, together with control of the impurity influx as envisaged for the JET pumped divertor, should yield higher values of Q_{DT}.

The techniques used for introducing, tracking, monitoring and recovering tritium have been demonstrated to be highly effective. Essentially all of the tritium introduced into the NB system has been recovered and, so far, about two thirds of that introduced into the torus. The remaining levels are sufficiently low for the JET experimental programme in deuterium to continue normally. The wall tiles will be removed at the start of the next shutdown, and post-mortem analysis should provide important data for the choice of wall materials for a next step device.

The transient nature of the type of H-mode discharge used for the deuterium–tritium experiment emphasizes the need to control the 'carbon bloom' and to develop a viable mode of operation for a reactor. Controlling the plasma exhaust and the ingress of impurities released at the divertor plates will be the major theme of the JET programme up to 1995. These data, together with those on tritium retention, will allow the planning of an effective campaign of deuterium–tritium experiments in 1996. These experiments will form the basis for accurate extrapolations to a next step device, i.e. to a device designed to operate routinely at a temperature sustained by its own fusion power.

Appendix

FUSION REACTIONS

The nuclear fusion reactions that are considered in this paper are:

$$D + D \rightarrow T\ [1.01\ MeV] + p\ [3.02\ MeV] \qquad (A.1a)$$

$$D + D \rightarrow {}^3He\ [0.82\ MeV] + n\ [2.45\ MeV] \qquad (A.1b)$$

$$D + T \rightarrow {}^4He\ [3.56\ MeV] + n\ [14.03\ MeV] \qquad (A.2)$$

The neutrons produced in reactions (A.1b) and (A.2) are referred to as 2.5 MeV and 14 MeV neutrons.

In evaluating the fusion power release and the fusion amplification factor Q (Section 5), 17.6 MeV energy per reaction has been used for Eq. (A.2) and 7.3 MeV per neutron released has been used for Eq. (A.1).

In a reactor, tritium would be regenerated by the capture of some neutrons in a lithium blanket, principally by the reaction:

$$n + {}^6Li \rightarrow {}^4He\ [2.1\ MeV] + T\ [2.7\ MeV] \qquad (A.3)$$

thereby releasing a further 4.8 MeV.

REFERENCES

[1] The JET Team, The JET Project — Design Proposal, Rep. EUR-JET-R5, CEC, Brussels (1975).

[2] The JET Team, Plasma Phys. Control. Fusion **32** (1990) 1083.

[3] JET Team, in Plasma Physics and Controlled Nuclear Fusion Research 1990 (Proc. 13th Int. Conf. Washington, DC, 1990), Vol. 1, IAEA, Vienna (1991) 27.

[4] The JET Team, Plasma Phys. Control. Fusion **33** (1991) 1453.

[5] REICHLE, R., CLEMENT, S., GOTTARDI, N., et al., in Controlled Fusion and Plasma Physics (Proc. 18th Eur. Conf. Berlin, 1991), Vol. 15C, Part III, European Physical Society (1991) 105.

[6] REBUT, P.-H., LALLIA, P.P., KEEN, B.E., in Fusion Engineering (Proc. 13th Symp. Knoxville, TN, 1989), Vol. 1, IEEE, Piscataway, NJ (1989) 227.

[7] STUBBERFIELD, P.M., BALET, B., CORDEY, J.G., Plasma Phys. Control. Fusion **33** (1991) 1255.
[8] WAGNER, F., BECKER, G., BEHRINGER, K., et al., Phys. Rev. Lett. **49** (1982) 1408.
[9] BARNES, M.R., GIBSON, A., Vacuum **18** (1968) 451.
[10] KEILHACKER, M.M., ENGELHARDT, W.W., STOTT, P.E., WATKINS, M.L., Review of Diagnostic Systems 1986, Rep. JET-IR-(86)16, JET Joint Undertaking, Abingdon, Oxfordshire (1986).
[11] GOLDSTON, R.J., McCUNE, D.C., TOWNER, H.H., et al., J. Comput. Phys. **43** (1981) 61.
[12] STORK, D., CAMPBELL, D.J., CLEMENT, S., et al., in Controlled Fusion and Plasma Physics (Proc. 18th Eur. Conf. Berlin, 1991), Vol. 15C, Part I, European Physical Society (1991) 357.
[13] EHRENBERG, J., J. Nucl. Mater. **145-147** (1987) 551.

(Manuscript received 20 December 1991
Final manuscript received 3 January 1992)

ANNEX

P.-H. REBUT, A. GIBSON, M. HUGUET, J.M. ADAMS[1], B. ALPER, H. ALTMANN, A. ANDERSEN[2], P. ANDREW[3], M. ANGELONE[4], S. ALI-ARSHAD, P. BAIGGER, W. BAILEY, B. BALET, P. BARABASCHI, P. BARKER, R. BARNSLEY[5], M. BARONIAN, D.V. BARTLETT, L. BAYLOR[6], A.C. BELL, G. BENALI, P. BERTOLDI, E. BERTOLINI, V. BHATNAGAR, A.J. BICKLEY, D. BINDER, H. BINDSLEV[2], T. BONICELLI, S.J. BOOTH, G. BOSIA, M. BOTMAN, D. BOUCHER, P. BOUCQUEY, P. BREGER, H. BRELEN, H. BRINKSCHULTE, D. BROOKS, A. BROWN, T. BROWN, M. BRUSATI, S. BRYAN, J. BRZOZOWSKI[7], R. BUCHSE[22], T. BUDD, M. BURES, T. BUSINARO, P. BUTCHER, H. BUTTGEREIT, C. CALDWELL-NICHOLS, D.J. CAMPBELL, P. CARD, G. CELENTANO, C.D. CHALLIS, A.V. CHANKIN[8], A. CHERUBINI, D. CHIRON, J. CHRISTIANSEN, P. CHUILON, R. CLAESEN, S. CLEMENT, E. CLIPSHAM, J.P. COAD, I.H. COFFEY[9], A. COLTON, M. COMISKEY[10], S. CONROY, M. COOKE, D. COOPER, S. COOPER, J.G. CORDEY, W. CORE, G. CORRIGAN, S. CORTI, A.E. COSTLEY, G. COTTRELL, M. COX[11], P. CRIPWELL[12], O. Da COSTA, J. DAVIES, N. DAVIES, H. de BLANK, H. de ESCH, L. de KOCK, E. DEKSNIS, F. DELVART, G.B. DENNE-HINNOV, G. DESCHAMPS, W.J. DICKSON[13], K.J. DIETZ, S.L. DMITRENKO, M. DMITRIEVA[14], J. DOBBING, A. DOGLIO, N. DOLGETTA, S.E. DORLING. P.G. DOYLE, D.F. DÜCHS, H. DUQUENOY, A. EDWARDS, J. EHRENBERG, A. EKEDAHL, T. ELEVANT[7], S.K. ERENTS[11], L.G. ERIKSSON, H. FAJEMIROKUN[12], H. FALTER, J. FREILING[15], F. FREVILLE, C. FROGER, P. FROISSARD, K. FULLARD, M. GADEBERG, A. GALETSAS, T. GALLAGHER, D. GAMBIER, M. GARRIBBA, P. GAZE, R. GIANNELLA, R.D. GILL, A GIRARD, A. GONDHALEKAR, D. GOODALL[11], C. GORMEZANO, N.A. GOTTARDI, C. GOWERS, B.J. GREEN, B. GRIEVSON, R. HAANGE, A. HAIGH, C.J. HANCOCK, P.J. HARBOUR, T. HARTRAMPF, N.C. HAWKES[11], P. HAYNES[11], J.L. HEMMERICH, T. HENDER[11], J. HOEKZEMA, D. HOLLAND, M. HONE, L. HORTON, J. HOW, M. HUART, I. HUGHES, T.P. HUGHES[10], M. HUGON, Y. HUO[16], K. IDA[17], B. INGRAM, M. IRVING, J. JACQUINOT, H. JAECKEL, J.F. JAEGER, G. JANESCHITZ, Z. JANKOVICZ[18], O.N. JARVIS, F. JENSEN, E.M. JONES, H.D. JONES, L.P.D.F. JONES, S. JONES[19], T.T.C. JONES, J.-F. JUNGER, F. JUNIQUE, A. KAYE, B.E. KEEN, M. KEILHACKER, G.J. KELLY, W. KERNER, A. KHUDOLEEV[21], R. KONIG, A. KONSTANTELLOS, M. KOVANEN[20], G. KRAMER[15], P. KUPSCHUS, R. LÄSSER, J.R. LAST, B. LAUNDY, L. LAURO-TARONI, M. LAVEYRY, K. LAWSON[11], M. LENNHOLM, J. LINGERTAT[22], R.N. LITUNOVSKI, A. LOARTE, R. LOBEL, P. LOMAS, M. LOUGHLIN, C. LOWRY, J. LUPO, A.C. MAAS[15], J. MACHUZAK[19], B. MACKLIN, G. MADDISON[11], C.F. MAGGI[23], G. MAGYAR, W. MANDL[22], V. MARCHESE, G. MARCON, F. MARCUS, J. MART, D. MARTIN, E. MARTIN, R. MARTIN-SOLIS[24], P. MASSMANN, G. MATTHEWS, H. McBRYAN, G. McCRACKEN[11], J. McKIVITT, P. MERIGUET, P. MIELE, A. MILLER, J. MILLS, S.F. MILLS, P. MILLWARD, P. MILVERTON, E. MINARDI[4], R. MOHANTI[25], P.L. MONDINO, D. MONTGOMERY[26], A. MONTVAI[27], P. MORGAN, H. MORSI, D. MUIR, G. MURPHY, R. MYRNÄS[28], F. NAVE[29], G. NEWBERT, M. NEWMAN, P. NIELSEN, P. NOLL, W. OBERT, D. O'BRIEN, J. ORCHARD, J. O'ROURKE, R. OSTROM, M. OTTAVIANI, M. PAIN, F. PAOLETTI, S. PAPASTERGIOU, W. PARSONS, D. PASINI, D. PATEL, A. PEACOCK, N. PEACOCK[11], R.J.M. PEARCE, D. PEARSON[12], J.F. PENG[16], R. PEPE DE SILVA, G. PERINIC, C. PERRY, M. PETROV[21], M.A. PICK, J. PLANCOULAINE, J.-P POFFÉ, R. PÖHLCHEN, F. PORCELLI, L. PORTE[13], R. PRENTICE, S. PUPPIN, S. PUTVINSKII[8], G. RADFORD[30], T. RAIMONDI, M.C. RAMOS DE ANDRADE, R. REICHLE, J. REID, S. RICHARDS, E. RIGHI, F. RIMINI, D. ROBINSON[11], A. ROLFE, R.T. ROSS, L. ROSSI, R. RUSS, P. RUTTER, H.C. SACK, G. SADLER, G. SAIBENE, J.L. SALANAVE, G. SANAZZARO, A. SANTAGIUSTINA, R. SARTORI, C. SBORCHIA, P. SCHILD, M. SCHMID, G. SCHMIDT[31], B. SCHUNKE, S.M. SCOTT, L. SERIO, A SIBLEY, R. SIMONINI, A.C.C. SIPS, P. SMEULDERS, R. SMITH, R. STAGG, M. STAMP, P. STANGEBY[3], R. STANKIEWICZ[32], D.F. START, C.A. STEED, D. STORK, P.E. STOTT, P. STUBBERFIELD, D. SUMMERS, H. SUMMERS[13], L. SVENSSON, J.A. TAGLE[33], M. TALBOT, A. TANGA, A. TARONI, C. TERELLA, A TERRINGTON, A TESINI, P.R. THOMAS, E. THOMPSON, K. THOMSEN, F. TIBONE, A. TISCORNIA, P. TREVALION, B. TUBBING, P. VAN BELLE, H. VAN DER BEKEN, G. VLASES, M. VON HELLERMANN, T. WADE, C. WALKER, R. WALTON[31], D. WARD, M.L. WATKINS, N. WATKINS, M.J. WATSON, S. WEBER[34], J. WESSON, T.J. WIJNANDS, J. WILKS, D. WILSON, T. WINKEL, R. WOLF, D. WONG, C. WOODWARD, Y. WU[35], M. WYKES, D. YOUNG, I.D. YOUNG, L. ZANNELLI, A. ZOLFAGHARI[19], W. ZWINGMANN

[1] Harwell Laboratory, UKAEA, Harwell, Didcot, Oxfordshire, UK.
[2] Risø National Laboratory, Roskilde, Denmark.
[3] Institute for Aerospace Studies, University of Toronto, Downsview, Ontario, Canada.
[4] ENEA Frascati Energy Research Centre, Frascati, Rome, Italy.
[5] University of Leicester, Leicester, UK.
[6] Oak Ridge National Laboratory, Oak Ridge, TN, USA.
[7] Royal Institute of Technology, Stockholm, Sweden.
[8] I.V. Kurchatov Institute of Atomic Energy, Moscow, Russian Federation.
[9] Queens University, Belfast, UK.
[10] University of Essex, Colchester, UK.
[11] Culham Laboratory, UKAEA, Abingdon, Oxfordshire, UK.
[12] Imperial College of Science, Technology and Medicine, University of London, London, UK.
[13] University of Strathclyde, Glasgow, UK.
[14] Keldysh Institute of Applied Mathematics, Moscow, Russian Federation.
[15] FOM-Institute for Plasma Physics "Rijnhuizen", Nieuwegein, Netherlands.
[16] Institute of Plasma Physics, Academia Sinica, Hefei, Anhui Province, China.
[17] National Institute for Fusion Science, Nagoya, Japan.
[18] Soltan Institute for Nuclear Studies, Otwock/Świerk, Poland.
[19] Plasma Fusion Center, Massachusetts Institute of Technology, Boston, MA, USA.
[20] Nuclear Engineering Laboratory, Lappeenranta University, Finland.
[21] A.F. Ioffe Physico-Technical Institute, St. Petersburg, Russian Federation.
[22] Max-Planck-Institut für Plasmaphysik, Garching, Germany.
[23] Department of Physics, University of Milan, Milan, Italy.
[24] Universidad Complutense de Madrid, Madrid, Spain.
[25] North Carolina State University, Raleigh, NC, USA.
[26] Dartmouth College, Hanover, NH, USA.
[27] Central Research Institute for Physics, Budapest, Hungary.
[28] University of Lund, Lund, Sweden.
[29] Laboratorio Nacional de Engenharia e Tecnologia Industrial, Sacavem, Portugal.
[30] Institute of Mathematics, University of Oxford, Oxford, UK.
[31] Princeton Plasma Physics Laboratory, Princeton University, Princeton, NJ, USA.
[32] RCC Cyfronet, Otwock/Świerk, Poland,
[33] Centro de Investigaciones Energéticas, Medioambientales y Tecnológicas, Madrid, Spain.
[34] Freie Universität, Berlin, Germany.
[35] Insitute for Mechanics, Academia Sinica, Beijing, China.